Cancer Chemother Pharmacol (1993) 32: 143–150

Cancer Chemotherapy and Pharmacology

Disposition and metabolism of KW-2149, a novel anticancer agent

S. Kobayashi, J. Ushiki, K. Takai, S. Okumura, M. Kono, M. Kasai, K. Gomi, M. Morimoto, H. Ueno, T. Hirata

Pharmaceutical Research Laboratories, Kyowa Hakko Kogyo Co., Ltd. Shizuoka, Japan

Received 20 April 1992/Accepted 29 December 1992

Abstract. KW-2149 is a new derivative of mitomycin C (MMC). The plasma concentrations, distribution, metabolism, and excretion of [^{3}H]-KW-2149 in normal and tumor-bearing mice after i.v. administration of 16.6 mg/kg were investigated. The plasma radioactivity decreased biexponentially after i.v. administration in normal mice. However, the unchanged drug disappeared rapidly, showing a half-life ($t_{1/2}$) of 9.7 min, which was shorter than MMC's (18 min). The radioactivity was excreted in mouse urine (33%) and feces (58%) within 144 h. High radioactivity was distributed in the gallbladder, liver, kidney, pancreas, and lung at 1 h after i.v. administration to normal mice. The tumor concentration was lower than the plasma or blood concentration. The lowest radioactivity was observed in the brain. The metabolic rate of KW-2149 was very rapid. The methyl sulfide form (M-16), the symmetrical disulfide dimer (M-18), and the albumin conjugate were detected in plasma, which possessed anticellular activity. The specific anticellular activity of these compounds against uterine carcinoma (HeLa S3) was 1/100, 1, and 1/20 respectively, as compared with that of KW-2149.

Introduction

Mitomycin C (MMC), an antitumor antibiotic, is currently used in the treatment of various tumors [5, 11]. In spite of its high antitumor activity, its clinical usefulness has been limited primarily by myelosuppression classified as leukopenia or thrombopenia. Therefore, new MMC analogues of MMC have been extensively investigated for many years, including the analogues with substituents at the 7-N position [2–4, 9], because N-7 has a strong association with the reduction of the quinone ring. We synthesized various MMC derivatives at N-7, one of which was 7-*N*-{{2-{[2-(γ-glutamylamino)ethyl]dithio}ethyl}}mitomycin C (KW-2149) [6]. KW-2149 exhibits potent antitumor activity against a variety of animal neoplasms and human tumor xenografts and has a highly cytotoxic effect on various cultured tumor cells in vitro. In addition, this drug is active against MMC-resistant P388 leukemia [8, 10].

In the present study, we investigated the plasma concentrations, excretion, distribution, and metabolism of KW-2149 following its i.v. administration to normal and tumor-bearing mice.

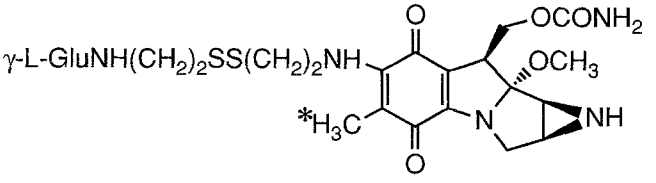

Fig. 1. Chemical structure of [^{3}H]-KW-2149. The *asterisk* indicates the tritium-labeled position

Materials and methods

Chemicals. [C6-CH$_2$^{3}H]KW-2149 ([^{3}H]-KW-2149, Fig. 1), 7-*N*-[2-(methylthio)-ethyl]mitomycin C (metabolite M-16), and 7-*N*,7′-*N*′-dithiodiethylenedimitomycin C (metabolite M-18) were synthesized in our laboratories. KW-2149 was synthesized in our Sakai plant (Osaka, Japan). The specific activity of [^{3}H]-KW-2149 was 20.2 GBq/mmol (0.547 Ci/mmol). Its chemical and radiochemical purity was determined by high-performance liquid chromatography (HPLC) using a YMC packed column AM312(ODS) (15 cm × 6 mm inside diameter; particle size, 5 μm; YMC, Kyoto, Japan) [eluents: 20% methanol (A) and 70% methanol (B); elution: 10-min linear gradient from 0 to 60% B, followed by 10-min linear gradient from 60% to 80% B; flow rate: 1 ml/min]. The

Abbreviations: MMC, mitomycin C; LD_{10}, 10% lethal dose; HPLC, high-performance liquid chromatography; AUC, area under the concentration-time curve; $t_{1/2}$, half-life; Vd_{ss}, volume of distribution at steady state; Cl_{tot}, total clearance

Correspondence to: Satoshi Kobayashi, Pharmaceutical Research Laboratories, Kyowa Hakko Kogyo Co., Ltd., 1188 Shimotogari, Nagaizumi-cho, Shizuoka 411, Japan

results were 97.8% and 97.9%. Porfiromycin was obtained from our medicinal chemistry laboratory and was used as the internal standard (IS) in quantitative HPLC. Oxidized glutathione (GSSG) was obtained from our Hofu plant (Yamaguchi, Japan). All other reagents and solvents were of analytical grade.

Animals and tumors. Male CDF1 strain mice (5 weeks old; body weight, 20–22 g) obtained from Japan SLC Inc. (Shizuoka, Japan) were used. The tumor-bearing CDF1 mice were 6 weeks old at experiment (body weight, 24–26 g) and were inoculated with tumor cells at the age of 5 weeks. The animals were housed under conditions of controlled temperature and lighting (12 h) and had free access to food (F-2; Funabashi Farms, Chiba, Japan) and water at all times. All animal experiments were carried out on three mice in a group. Murine lymphocytic P388 leukemia was kindly supplied by the National Cancer Institute (Bethesda, Md., USA). MMC-resistant P388 leukemia (P388/MMC) was kindly supplied by Dr. M. Inaba, Japanese Foundation for Cancer Research (Tokyo, Japan). In experiments, P388 (1×10^6) or P388/MMC (1×10^6) cells were inoculated s. c. into the flank of 5-week-old mice.

Animal experiments. For the study of plasma and blood concentrations, [^{3}H]-KW-2149 was dissolved in physiological saline and injected i. v. into mice (100–110 μCi/kg; 16.6 mg/kg). Animals were gang-housed in standard cages. The blood and plasma were collected at appropriate points until 144 h after dosing.

For the study of urinary and fecal excretion, [^{3}H]-KW-2149 was given i. v. to mice (120–130 μCi/kg; 16.6 mg/kg). The animals were housed in individual metabolism cages to permit separation and collection of urine and feces. Urine and feces were collected at appropriate intervals until 144 h after dosing.

For the study of tissue distribution, the animals were killed by abscission of the carotid arteries at appropriate times following the i. v. administration of [^{3}H]-KW-2149 (80–200 μCi/kg; 16.6 mg/kg). Tissues and tumor were rapidly excised, washed in saline, and weighed. About 100 mg was taken from each tissue and dried. In the case of small amounts of tissue (<100 mg), the whole tissue was dried.

For studies of the plasma concentration-time profile of KW-2149 and its metabolites and the anticellular activity concentration-time profile, unlabeled KW-2149 was injected i. v. into mice (16.6 mg/kg). Blood was collected at appropriate times after dosing.

In another experiment, unlabeled KW-2149 was given i. v. to male Wistar rats (250–300 g; Nihon Rat Co. Ltd., Saitama, Japan) to obtain larger amounts of plasma metabolites (dose, 16.6 mg/kg).

Radiochemical analysis. Radioactivity was measured in a liquid scintillation counter (Tri-Carb 300; Packard, Ill., USA) after combusting of dried samples by means of an automatic sample oxidizer (Tri-Carb 306, Packard). All counts were corrected for quenching by the automatic external standardization method. Only in the case of feces was the homogenate with saline treated in the same manner after drying.

Determination of unchanged KW-2149 and its metabolites in plasma. We have previously found that KW-2149 reacts very rapidly with SH groups in biological fluid components, including albumin, glutathione, and others; that is, KW-2149 was not observed after incubation in 4% human serum albumin at 37° C for 1 day (30 μg/ml, pH 7.4). *N*-Ethylmaleimide (an SH-blocking agent) inhibited the reaction completely (unpublished data). Prior to the HPLC assay, we treated the blood with GSSG (final concentration, 4%) to inhibit the reaction of KW-2149 with SH groups in the blood.

KW-2149 and its metabolites [except the KW-2149-albumin conjugate (albumin conjugate)] in GSSG-treated plasma were assayed using reverse-phase HPLC after they had been extracted from the biological matrix by solid-phase extraction. Following the addition of porfiromycin (IS), the plasma was applied to a solid-phase extraction column (Bond Elut C8; Analytichem International, Calif., USA) that had previously been activated with 3 ml methanol and 3 ml water. After a washing step with 20% methanol (2 ml), KW-2149, IS, and KW-2149 metabolites were eluted with methanol (2 ml × 2). The eluate was dried to allow for concentration of the sample. The residue was reconstituted with the HPLC mobile phase.

Chromatography was performed on a reverse-phase column (YMC packed column AQ312; 15 cm × 6 mm inside diameter; particle size, 10 μm; YMC) at room temperature. Solvent A was 0.05 *M* phosphate buffer (pH 7.0)-acetonitrile (82 : 18, v/v) containing 5 m*M* sodium octanesulfonate, and solvent B was 0.05 *M* phosphate buffer (pH 7.0)-acetonitrile (50 : 50, v/v) containing 5 m*M* sodium octanesulfonate. The solvents were degassed by vacuum and ultrasound. The flow rate was set at 1 ml/min and the detection wavelength, at 375 nm. For elution, the first linear gradient from 0 to 30% solvent B was applied until 15 min, and the second linear gradient from 30% to 100% solvent B followed the first gradient until 30 min. The retention times of KW-2149, M-16, M-18, and porfiromycin (IS) were 16, 26, 30, and 11 min, respectively. Quantitation was possible down to 2 ng KW-2149/ml using 0.5 ml plasma. The metabolite concentration was expressed as the KW-2149 equivalent.

Albumin conjugate in plasma was also assayed using reverse-phase HPLC by direct injection. Chromatography was performed at room temperature on the same column described above. Solvent A was 0.05% trifluoroacetic acid (TFA)-acetonitrile (90 : 10, v/v), and solvent B was 0.05% TFA-acetonitrile (40 : 60, v/v). The flow rate was set at 1 ml/min and the detection wavelength, at 375 nm. For elution, a linear gradient from 0 to 100% solvent B was applied until 60 min. The retention time of albumin conjugate was 42 min. The quantitation was done using the absolute-calibration curve method. Since we had no reference of albumin conjugate, its concentration was determined as the KW-2149 equivalent.

Isolation of metabolites. To obtain a large amount of each metabolite, we gave KW-2149 i. v. to rats (16.6 mg/kg). Whole blood was taken from the external iliac artery and vein into heparinized tubes at 5 min after i. v. administration. The blood was centrifuged to separate the plasma. After extraction using a Bond-Elut column, the eluate was separated on a semipreparative reverse-phase column [YMC packed column S-343-15 (ODS); 25 cm × 20 mm inside diameter; particle size, 15 μm; YMC). Solvent A was 20 m*M* CH_3COONH_4-methanol (70 : 30, v/v), and solvent B was 20 m*M* CH_3COONH_4-methanol (7 : 93, v/v). For elution, a linear gradient from 0 to 100% solvent B was employed until 60 min. The flow rate was set at 9.9 ml/min and the detection wavelength, at 375 nm.

Spectroscopy. Fast atom bombardment (FAB) mass spectra were measured with a JMS-D-300 mass spectrometer (JEOL Ltd. Tokyo, Japan). The accelerating voltage was 5 keV. [^{1}H]-Nuclear magnetic resonance (NMR) spectra were measured with a GSX-270 NMR spectrometer (JEOL Ltd.). Samples were dissolved in $CDCl_3$, with tetramethylsilane (TMS) serving as the internal standard.

Anticellular activity. HeLa S3 cells were precultured for 24 h in a 96-well microplate (Nunc, Roskilde, Denmark) containing 0.1 ml of the culture medium at 37° C in a humidified atmosphere containing 5% CO_2 in air. The cells were then treated with the drug-containing sample (not GSSG-treated) for 1 h, washed, and further incubated in drug-free culture medium for 72 h at 37° C. The anticellular activity of the sample was evaluated by the inhibition of neutral red dye uptake into the cells. Briefly, after the incubation, the culture medium was discarded and 0.1 ml 0.02% (w/v) neutral red-containing medium was added to each well. After a 1-h incubation, the solution was discarded and each well was washed with 0.1 ml 0.9% (w/v) NaCl solution. The neutral red dye was extracted by 0.1 ml 30% (v/v) ethanol solution with 0.001 *N* HCl, and the absorbance at 550 nm was measured on a microplate reader (Corona Electric Co., Ibaragi, Japan).

Pharmacokinetic analysis. Pharmacokinetic parameters were calculated using model-independent methods [1]. The terminal rate constant was determined by log-linear regression analysis of the terminal phase of the blood/plasma concentration-time curves. The terminal blood/plasma half-lives were calculated by half-life equals 0.693/terminal rate constant. The area under the concentration-time curve (AUC) and the area under the first-moment curves (AUMC) were calculated by the trapezoidal rule with extrapolation to infinity. The mean residence time

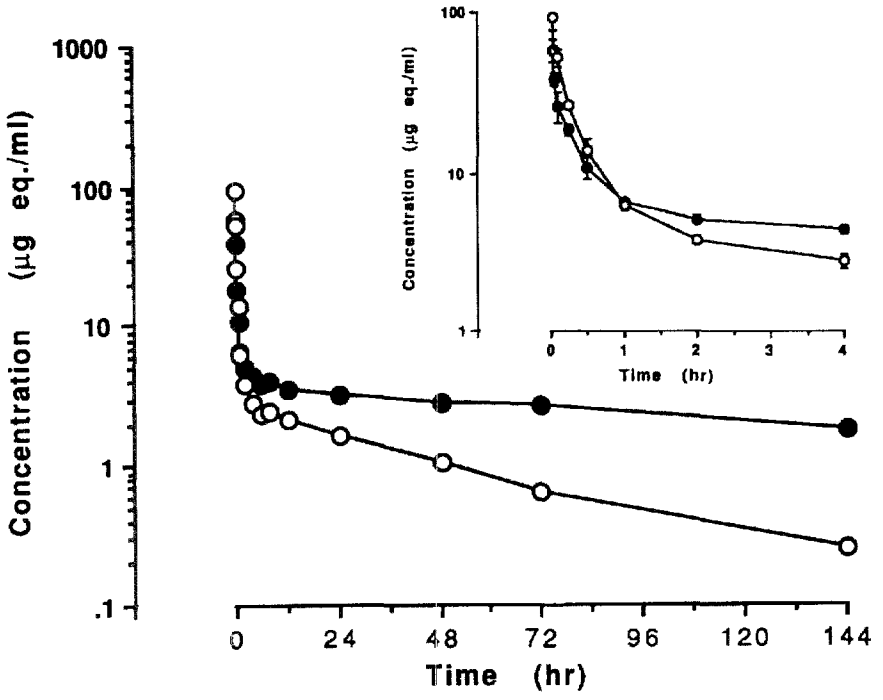

Fig. 2. Blood and plasma concentration of radioactivity after i. v. administration of [^{3}H]-KW-2149 in normal mice (16.6 mg/kg). ●——●, Blood concentration; ○——○, plasma concentration; *points*, mean values; *bars*, SD ($n = 3$)

Table 1. Pharmacokinetic parameters of radioactivity after i. v. administration of 16.6 mg/kg [^{3}H]-KW-2149 to normal mice

Parameter		Blood	Plasma
$t_{1/2\alpha}$	(h)	0.197	0.211
$t_{1/2\beta}$	(h)	147	44.9
MRT	(h)	205	51.2
Vd_{ss}	(ml/kg)	4310	4810
Cl_{tot}	(ml kg^{-1} h^{-1})	21.0	93.9
$AUC_{0-\infty}$	(μg eq h ml^{-1})	792	177

Mean values ($n = 3$)

Table 2. Cumulative excretion of radioactivity in urine and feces after i. v. administration of 16.6 mg/kg [^{3}H]-KW-2149 to normal mice

Time (h)	Excreted radioactivity (% of dose)	
	Urine	Feces
0– 6	22.5 ± 7.8[a]	–[b]
0– 12	29.1 ± 1.5	–
0– 24	30.8 ± 1.1	53.7 ± 1.9
0– 48	31.7 ± 1.1	56.3 ± 2.0
0– 72	32.2 ± 1.0	57.1 ± 2.1
0–144	32.9 ± 0.9	57.7 ± 2.2

Total excretion of radioactivity for 144 h was 90.6% of the dose
[a] Mean values ± SD ($n = 3$)
[b] Not collected

(MRT) was calculated by dividing the AUMC by the AUC. Total plasma clearance (Cl_{tot}) was calculated by dividing the dose by the AUC extrapolated from zero to infinity. The apparent distribution volume at steady state (Vd_{ss}) was determined by the following equation:

$Vd_{ss} = Cl_{tot} \times MRT$.

Results

Blood and plasma concentrations of radioactivity

The plasma and blood radioactivity-concentration profile after the i.v. administration of [^{3}H]-KW-2149 to normal mice (16.6 mg/kg) is shown in Fig. 2. The data represent mean values for three animals and were calculated as microgram equivalents of KW-2149 per milliliter. Since these values were based on total drug-related radioactivity, they represent the sum of both KW-2149 and its metabolites in the samples. The plasma concentrations observed at the first sampling time (1 min after administration) ranged from 76.2 to 108.4 μg eq/ml. The radioactivity diminished rapidly from the plasma, with the concentrations observed at 30 min being approximately 10%–20% of those measured at the initial sampling time. At 1 h, the plasma concentrations ranged from 5.73 to 6.66 μg eq/ml, which represented approximately 7% of the concentration measured at 1 min. Figure 2 shows the very rapid clearance of radioactivity from plasma during the early phase (0–1 h), followed by a very long shallow phase (1–144 h) during which slower elimination occurred. The pharmacokinetic parameters of radioactivity in plasma (blood) were calculated by model-independent analysis. The pharmacokinetic parameters are summarized in Table 1.

Excretion radioactivity

The amounts of radioactivity excreted in urine and feces after the i.v. administration of [^{3}H]-KW-2149 to normal mice are summarized in Table 2. The majority of the administered radioactivity was excreted in feces (57.7%)

Table 3. Tissue distribution of radioactivity after i.v. administration of 16.6 mg/kg [^{3}H]-KW-2149 to normal mice

Tissue	Concentration (μg eq of KW-2149/ml or g)			
	15 min	1 h	4 h	24 h
Plasma	26.58± 1.05[a]	6.29± 0.49	2.80± 0.28	1.62±0.09
Blood	18.59± 1.30	6.54± 0.25	4.41± 0.26	3.19±0.28
Brain	0.61± 0.03	0.32± 0.07	0.10± 0.03	0.08±0.01
Eyeball	4.19± 0.20	2.04± 0.21	1.13± 0.14	0.88±0.03
Thymus	6.52± 0.79	2.55± 0.53	0.99± 0.12	0.81±0.15
Heart	7.97± 0.45	2.97± 0.30	1.44± 0.08	1.04±0.10
Lung	18.16± 1.63	7.36± 0.43	3.90± 0.15	2.85±0.33
Liver	53.48± 1.69	25.05± 4.23	13.58± 0.66	6.17±0.60
Gallbladder	266.47±84.16	138.69±38.43	592.54±264.63	5.66±2.67
Kidney	23.89± 2.34	15.80± 1.68	7.72± 1.69	4.30±0.39
Adrenal gland	11.26± 0.69	2.05± 1.81	1.61± 0.11	1.00±0.26
Pancreas	7.59± 1.15	8.79± 2.24	1.06± 0.11	0.53±0.01
Spleen	5.80± 0.39	3.29± 0.62	2.01± 0.35	1.44±0.10
Testis	2.82± 0.36	1.60± 0.22	0.69± 0.07	0.36±0.02
Muscle	3.78± 0.50	3.32± 1.97	0.69± 0.07	0.46±0.04
Skin	10.12± 1.11	4.68± 0.53	1.50± 0.21	1.01±0.01
Fat	1.62± 0.04	3.86± 1.05	0.62± 0.43	0.17±0.02
Bone marrow	10.30± 5.88	4.50± 0.20	1.67± 0.59	2.22±0.54

[a] Mean values ± SD (n = 3)

Table 4. Tissue distribution of radioactivity after i.v. administration of 16.6 mg/kg [^{3}H]-KW-2149 to mice bearing P388 and P388/MMC tumors

Tumor	Tissue	Concentration (μg eq of KW-2149/ml or g)			
		15 min	1 h	4 h	24 h
P388	Plasma	32.45± 2.75[a]	17.07± 13.90	3.83± 1.20	1.49±0.13
	Brain	1.53± 0.08	0.79± 0.57	0.32± 0.08	0.12±0.02
	Lung	9.13± 1.56	6.22± 3.53	2.29± 0.26	1.47±0.18
	Liver	45.14± 1.44	19.25± 4.08	10.96± 1.65	5.18±0.19
	Gallbladder	135.35± 55.00	131.71± 61.09	86.54±26.73	6.56±1.33
	Kidney	50.38± 5.27	33.61± 8.96	17.54± 3.41	8.13±0.62
	Pancreas	25.89± 11.06	17.02± 11.83	11.34± 4.13	2.07±1.13
	Bone marrow	17.89± 7.43	10.65± 4.31	4.65± 1.98	2.22±0.23
	Tumor	15.10± 4.94	11.92± 3.32	4.99[b]	2.51±0.12
P388/MMC	Plasma	28.00± 2.48	6.86± 0.50	2.41± 0.13	1.18±0.13
	Brain	0.96± 0.13	0.37± 0.03	0.19± 0.03	0.14±0.02
	Lung	16.06± 2.09	5.77± 0.66	3.63± 0.58	2.41±0.32
	Liver	49.60± 3.90	24.53± 2.41	15.23± 3.36	7.88±0.27
	Gallbladder	198.38±112.69	309.70±252.42	267.36±47.87	9.59±0.84
	Kidney	33.22± 3.41	21.33± 2.31	11.65± 1.59	6.95±1.03
	Pancreas	11.11± 1.79	7.49± 2.67	3.50± 0.23	4.86±2.62
	Bone marrow	8.45± 0.44	3.39± 0.68	1.69± 0.38	2.30±0.05
	Tumor	6.56± 0.83	4.71± 0.69	3.23± 0.42	2.31±0.11

[a] Mean values ± SD (n = 3)
[b] Mean value (n = 2)

over 144 h, and the amount excreted in urine was 32.9% of the dose. Most of the fecal excretion (>92%) was recovered within 24 h after dosing, whereas the greater part of urinary recovery (>88%) was obtained within 12 h. The overall recovery in feces and urine averaged 90.6% of the dose.

Tissue distribution of radioactivity

The tissue concentrations of radioactivity measured after the i.v. administration of [^{3}H]-KW-2149 to normal and tumor-bearing mice are listed in Tables 3 and 4. The data represent mean values for three animals and were calculated as microgram equivalents of KW-2149 per gram or milliliter of wet tissue.

In normal mice (Table 3), the highest tissue concentrations of radioactivity were found in the gallbladder, liver, kidney, blood, and lung at almost all sampling intervals. These tissues had higher concentrations of radioactivity than did the plasma throughout the experiment. The tissues or organs that consistently showed lower concentrations of radioactivity were the brain, fat, testis, muscle, pancreas, and thymus. The lowest concentration was found in the

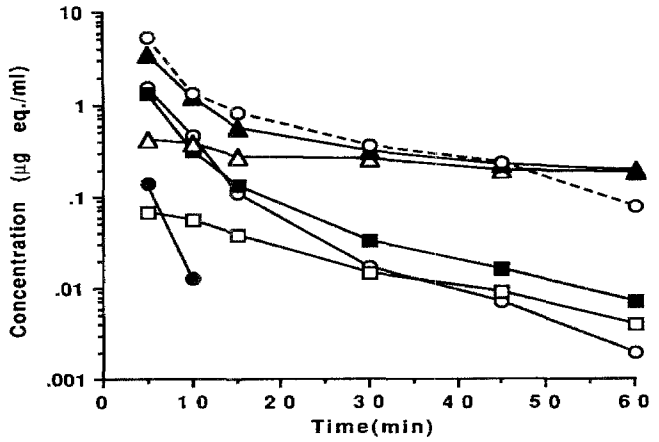

Fig. 3. Comparison between total anticellular activity and activity concentrations of KW-2149 and its metabolites after i. v. administration of 16.6 mg/kg KW-2149 to mice. O——O, KW-2149; ●——●, albo form; □——□, M-16; ■——■, M-18; △——△, albumin conjugate; ▲——▲, sum of KW-2149, albo form, M-16, M-18, and albumin conjugate; O------O, total anticellular activity; *points*, mean values

brain. The tissues from which radioactivity diminished most rapidly were the brain, fat, and gallbladder. However, the radioactivity concentration fell much slower in bone marrow during the 24-h period after dosing. The concentration in blood consistently exceeded that in plasma after 1 h.

In P388 tumor-bearing mice (Table 4), the highest tissue concentrations of radioactivity were observed in the gallbladder, kidney, liver, and blood at almost all sampling points. The concentration of radioactivity determined in the tumor (15.1 μg eq/g) was almost half of that detected in plasma at 15 min after dosing; however, it became 1.7-fold that in plasma at 24 h. In some tissues (kidney and pancreas), the elimination of radioactivity was slower than that observed in normal mice.

In P388/MMC tumor-bearing mice (Table 4), the highest tissue concentrations of radioactivity were observed in the gallbladder, liver, kidney, and blood at almost all sampling times. The concentration of radioactivity measured in the tumor (6.56 μg eq/g) was almost one-fourth of that determined in plasma at 15 min; however, it became 2-fold that in plasma at 24 h after dosing. In some tissues (kidney and pancreas), the elimination of radioactivity was slower than that observed in normal mice.

Isolation by preparative HPLC and mass spectral characterization of metabolites

The analytical system used for the determination of KW-2149, its albo form, and its metabolites was not a satisfactory method for preparative separation. A preparative separation system designed for performance under other conditions was developed. The flow rate and column dimension were increased to allow the preparative isolation of KW-2149 and its metabolites from rat plasma. We used the plasma of administered rats for the isolation of metabolites because we could not obtain sufficient quantities of metabolites from mouse plasma to perform their spectral analysis.

The isolated, purified samples were compared with the authentic samples of 7-*N*-[2-(methylthio)ethyl]mitomycin C and 7-*N*,7′-*N*′-dithiodiethylenedimitomycin C by HPLC, [^{1}H]-NMR, and FAB mass spectrometry.

The mass spectrum of 7-*N*-[2-(methylthio)ethyl]mitomycin C showed a characteristic ion at m/z 409, representing the adduct ion $[M+H]^+$. Several fragment ions were also observed. The spectrum of isolated M-16 showed excellent correspondence to the spectra for the adduct molecular ion and fragments, indicating that the M-16 isolated from plasma represents 7-*N*-[2-(methylthio)ethyl]mitomycin C. The mass spectrum of 7-*N*,7′-*N*′-dithiodiethylenedimitomycin C showed characteristic ions at m/z 787 and 788, representing the adduct ions $[M+H]^+$ and $[M+2H]^+$, respectively. Several fragment ions were also observed. The spectrum of isolated M-18 showed excellent correspondence to the spectra for the adduct molecular ions and fragments, indicating that the M-18 isolated from plasma represents 7-*N*,7′-*N*′-dithiodiethylenedimitomycin C.

We could not isolate enough of the albumin conjugate of KW-2149 for precise analysis. However, we observed that KW-2149 rapidly and extensively reacted with albumin in vitro at 37° C, since the KW-2149 peak shifted to the albumin fraction in gel-permeation HPLC monitoring the absorbance at 375 nm, which is characteristic for KW-2149.

Table 5. Pharmacokinetic parameters of KW-2149 and its metabolites in normal mice after i. v. administration of 16.6 mg/kg

Compound	T_{max} (min)	C_{max} (μg/ml)	$t_{1/2\alpha}$ (min)	$t_{1/2\beta}$ (min)	$AUC_{0-\infty}$ (μg min ml^{-1})	Metabolic ratio[a]
KW-2149			1.1[b]	9.7	110.6	
Albo form			1.5	ND	6.2	
M-16	3.0	6.6	–[c]	12.6	116.5	0.95
M-18	1.0	1.3	–	12.1	6.6	16.76
Alb.conj.[d]	1.0	4.6	–	40.3	296.6	0.37

[a] AUC of unchanged drug/AUC of metabolite
[b] Mean values ($n = 3$)
[c] Not calculated
[d] Albumin conjugate, values converted to KW-2149 equivalents
ND, Not detected

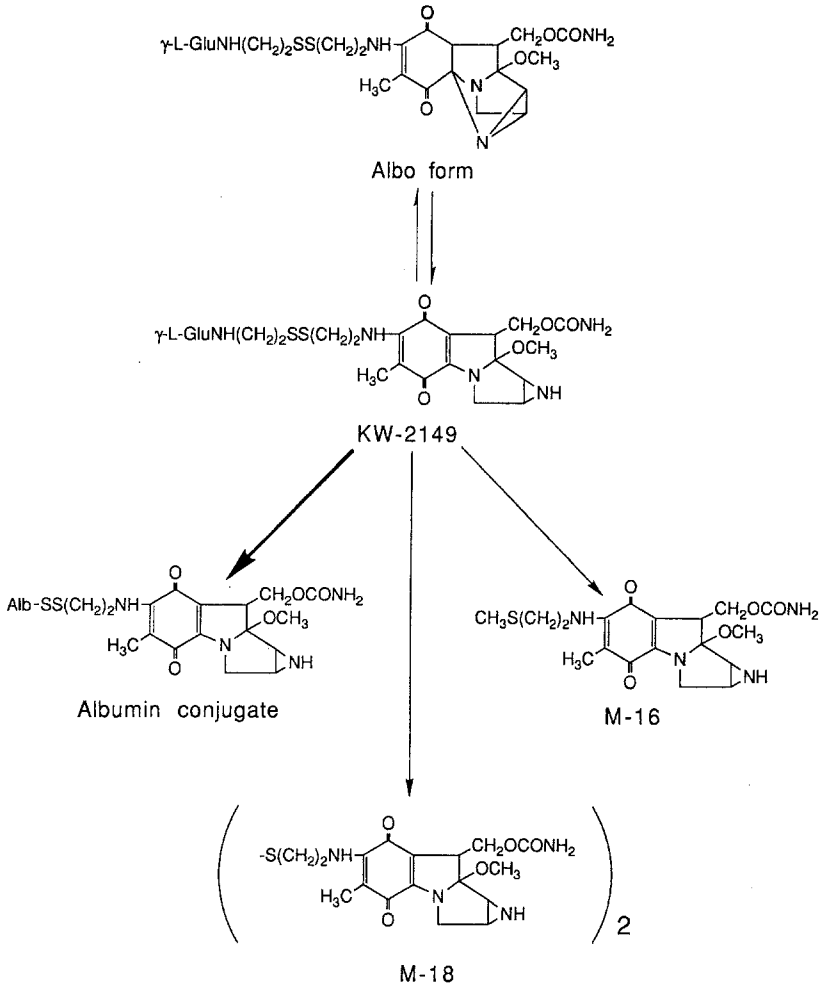

Fig. 4. Proposed metabolic pathways of KW-2149. *Alb*, Albumin

Separative determination of unchanged KW-2149, its albo form, and its metabolites in plasma

The plasma concentration-time profiles of KW-2149 and its metabolites were studied in normal mice after i.v. administration of the former. Plasma concentrations of KW-2149 decreased rapidly and biphasically, with the first elimination half-life being about 1 min and the second being about 10 min. The albo form of KW-2149, M-16, M-18, and the albumin conjugate were generated at once after dosing. The albo form, M-16, and M-18 were eliminated quickly, showing short half-lives (<13 min). In contrast, the albumin conjugate diminished gradually, displaying a half-life of about 40 min. The albumin conjugate showed the largest AUC, which was about 3 times greater than that of KW-2149 (Table 5).

Anticellular activity concentration in plasma

Anticellular activity concentrations in plasma after the i.v. administration of KW-2149 to normal mice were determined by an anticellular activity test using HeLa S3 cells (Fig. 3). Separately we determined the specific anticellular activity of each metabolite; that is to say, the specific anticellular activity of the albo form, M-16, M-18, and the albumin conjugate (as KW-2149) were 1, 1/100, 1, and 1/20, respectively. All plasma concentrations of metabolites determined by HPLC were converted to anticellular activity concentrations by specific anticellular activities. Total anticellular activity concentrations in plasma were almost in accord with the sum of converted anticellular activity concentrations of KW-2149, the albo form, M-16, M-18, and the albumin conjugate.

Discussion

It has been reported that KW-2149 shows potent activity against P388 leukemia as well as the L27 xenograft and is also effective against MMC-resistant P388 leukemia [8, 10]. The plasma (blood) concentrations, excretion, tissue (including tumor) distribution, and metabolism of the drug were investigated after the i.v. administration of [^{3}H]-KW-2149 (16.6 mg/kg, LD_{10}) to normal and tumor-bearing mice in the present study.

[^{3}H]-KW-2149 disappeared biphasically from plasma following its i.v. administration to normal mice, its plasma half-life being 44.9 h (β-phase). From 1 h after administration onward, the blood radioactivity concentration exceeded the plasma radioactivity concentration, suggesting the distribution of KW-2149 and its metabolites to

blood cells. The blood half-life of the β-phase was as long as 147 h. This indicates that the release of KW-2149 and metabolites taken up into blood cells is remarkably slow.

Within 144 h of administration, 33% of the [3H]-KW-2149 dose was excreted in the urine as compared with 58% in the feces. Thus, [3H]-KW-2149 was mainly excreted in the feces. The amount of radioactivity in the feces may be associated with the dose excreted via the bile and/or secreted directly through the gastrointestinal mucosa. Biliary excretion may be the main excretory route of [3H]-KW-2149, since we found the highest radioactivity concentration in the gallbladder.

Only in the gallbladder and liver was the radioactivity concentration higher than that measured in plasma at 15 min after [3H]-KW-2149 administration to normal mice. It is assumed that the tissue distribution of [3H]-KW-2149 is lower. In P388 tumor-bearing mice, the plasma radioactivity concentration-time profile was similar to that observed in normal mice. The distribution of [3H]-KW-2149 to the gallbladder and kidney was high, whereas the distribution to the liver was lower than that noted in normal mice. This phenomenon was of interest and characteristic in P388 tumor-bearing mice but was not encountered in P388/MMC tumor-bearing mice or L27 tumor-bearing mice. However, it remains to be determined whether this phenomenon was due to the change in liver function caused by the tumor.

In bone marrow, the tissue-to-plasma radioactivity concentration ratio was 0.3 at 15 min after i.v. administration of [3H]-KW-2149, when considerable amounts of unchanged drug were present. The low distribution of [3H]-KW-2149 in the bone marrow may be one of the causes of its low myelotoxicity. Since the radioactivity concentration in the brain was much lower in normal and tumor-bearing mice, it is assumed that it is hard for KW-2149 and its metabolites to permeate the blood-brain barrier.

The distribution of [3H]-KW-2149 to the tumor in P388 tumor-bearing mice was lower than that to plasma immediately after administration, whereas from 4 h after administration onward, the radioactivity concentration in the tumor was higher than that in plasma. The distribution to the tumor in P388/MMC tumor-bearing mice was lower than that in P388 tumor-bearing mice immediately after administration, whereas from 4 h onward, the tumor radioactivity concentrations were similar in both groups. It has been reported that KW-2149 is effective against MMC-resistant murine leukemia. However, this effectiveness could not be explained by the radioactivity concentration detected in the tumor in the present study. The concentrations of unchanged drug and active metabolites in the tumor should be studied.

Among the many metabolites detected in plasma, we first picked up the metabolites by antitumor activity and identified the albo form, M-16, M-18, and the albumin conjugate. The ratio of the antitumor activity of each metabolite to that of KW-2149 was 1, 1/100, 1, and 1/20 (as KW-2149), respectively. An HPLC system that could determine each metabolite quantitatively was developed, and metabolites as well as KW-2149 in plasma were determined after KW-2149 had been given i.v. to normal mice. The sum of the KW-2149 concentration and the anticellular activity concentrations of metabolites, which were converted by specific anticellular activities, corresponded very closely to the total anticellular activity concentration in plasma. Accordingly, it appeared that the anticellular activity in plasma could be explained by KW-2149 and these active metabolites. KW-2149 disappeared more rapidly from plasma, showing a half-life of 9.7 min as compared with 18 min for MMC (unpublished data), which demonstrates that its activity is superior to that of MMC against P388 leukemia, M5076 sarcoma, and B16 melanoma. The AUC of KW-2149 was only 1% of the total radioactivity AUC. Its metabolites were formed quickly, and M-16 and M-18 disappeared with the half-lives of 13 and 12 min, respectively. On the other hand, the albumin conjugate resided for long periods in plasma and disappeared slowly with a half-life of 40 min. Moreover, its AUC was about 3 times as large as that of the unchanged drug. It is assumed that the disappearance of the albumin conjugate results from its degradation by the SH/SS exchange reaction with SH groups (such as glutathione, cystein, and others), which occurs in the same way as its formation and digestion in the liver and kidney [7]. However, the participation of reducing enzymes cannot be excluded.

The very late elimination of radioactivity ($t_{1/2}$, 45–150 h) cannot be explained by these active metabolites. Thus, it is assumed that other metabolites exist with longer half-lives.

As a result of this study, the proposed metabolic pathways of KW-2149 are shown in Fig. 4. The participation of disulfide reductase, S-methyltransferase, and other enzymes that may play important roles in the cleavage of disulfide and the methylation of SH groups is under examination.

The novel MMC analogue KW-2149 exhibits activity superior to that of MMC. Furthermore, it appears that KW-2149 is converted to several active metabolites (M-16, M-18, albumin conjugate) by cleavage of the disulfide bond. Unlike MMC, the unchanged drug and active metabolites showed the sustenance of anticellular activity in plasma.

Acknowledgements. We thank H. Kikuchi and H. Ohno for their technical assistance.

References

1. Gibaldi M (1984) Noncompartmental pharmacokinetics. In: (eds) Biopharmaceutics and clinical pharmacokinetics, 3rd edn. Lea and Febiger, Philadelphia, p 17
2. Iyengar BS, Lin H-J, Cheng L, Remers WA (1981) Development of new mitomycin C and porfiromycin analogues. J Med Chem 24: 975
3. Iyengar BS, Sami SM, Remers WA, Bradner WT, Schurig JE (1983) Mitomycin C and porfiromycin analogues with substituted ethylamines at position 7. J Med Chem 26: 16
4. Iyengar BS, Sami SM, Tarnow SE, Remers WA, Bradner WT, Schurig JE (1983) Mitomycin C analogues with secondary amines at position 7. J Med Chem 26: 1453
5. Kinoshita S, Uzu K, Nakano K, Shimizu M, Takahashi T, Matsui M (1971) Mitomycin derivatives: I. Preparation of mitosane and mitosene compounds and their biological activities. J Med Chem 14: 103

6. Kono M, Saitoh Y, Kasai M, Sato A, Shirahata K, Morimoto M, Ashizawa T (1989) Synthesis and antitumor activity of a novel water soluble mitomycin analog; 7-*N*-{{2-{[2-(γ-L-glutamylamino)ethyl]-dithio}ethyl}}mitomycin C. Chem Pharm Bull (Tokyo) 37: 1128
7. Meijer DKF, Sluijs P van der (1989) Covalent and noncovalent protein binding of drugs: implications for hepatic clearance, storage, and cell-specific drug delivery. Pharm Res 6: 105
8. Morimoto M, Ashizawa T, Ohno H, Azuma M, Kobayashi E, Okabe M, Gomi K, Kono M, Saitoh Y, Kanda Y, Arai H, Sato A, Kasai M, Tsuruo T (1991) Antitumor activity of 7-*N*-{{2-{[2-(γ-L-glutamyl-amino)ethyl]dithio}ethyl}}-mitomycin C. Cancer Res 51: 110
9. Sami SM, Iyengar BS, Tarnow SE, Remers WA, Bradner WT, Schurig JE (1984) Mitomycin C analogues with aryl substituents on the 7-amino group. J Med Chem 27: 701
10. Tsuruo T, Sudo Y, Asami N, Inaba M, Morimoto M (1990) Antitumor activity of a derivative of mitomycin,7-*N*-[2-[[2-(γ-L-glutamylamino)ethyl]dithio]ethyl]mitomycin C (KW-2149), against murine and human tumors and a mitomycin C-resistant tumor in vitro and in vivo. Cancer Chemother Pharmacol 27: 89
11. Usubuchi I, Sobajima Y, Hongo T, Kawaguchi T, Sugawara M, Matsui M, Wakaki S, Uzu K (1967) Antitumor studies on mitomycin derivatives: 1. Effect on Hirosaki ascites sarcoma. Jpn J Cancer Res 58: 307